



Transition from Bose glass to a condensate of triplons in $\text{Tl}_{1-x}\text{K}_x\text{CuCl}_3$

Fumiko Yamada,¹ Hidekazu Tanaka,¹ Toshio Ono,¹ and Hiroyuki Nojiri²

¹*Department of Physics, Tokyo Institute of Technology, Meguro-ku, Tokyo 152-8551, Japan*

²*Institute for Material Research, Tohoku University, Aoba-ku, Sendai 980-8577, Japan*

(Received 14 June 2010; revised manuscript received 3 October 2010; published 21 January 2011)

We report the magnetic-field-induced Bose glass–Bose-Einstein condensate (BEC) transition of triplons in $\text{Tl}_{1-x}\text{K}_x\text{CuCl}_3$ and its critical behavior, which were investigated through specific heat and electron spin resonance (ESR) measurements. The field dependence of the BEC transition temperature T_N can be described by the power law $[H - H_c] \propto T_N^\phi$ near the quantum critical point $H_c \sim 3$ T. The critical exponent ϕ tends to reach a value smaller than $1/2$ with decreasing fitting window in contrast to $\phi \rightarrow 3/2$ for the standard BEC in a pure system. At sufficiently low temperatures, the ESR line shape for $H \simeq H_c$ is intermediate between Gaussian and Lorentzian functions. This implies the localization of triplons for $H < H_c$ at $T = 0$.

DOI: [10.1103/PhysRevB.83.020409](https://doi.org/10.1103/PhysRevB.83.020409)

PACS number(s): 75.10.Jm, 64.70.Tg, 75.40.Cx, 72.15.Rn

Heisenberg antiferromagnets composed of spin dimers often have gapped ground states and undergo quantum phase transitions to ordered states in magnetic fields.^{1,2} The field-induced magnetic ordering is typical of the quantum phase transition and has been actively studied both theoretically and experimentally.^{3–14} These studies have established that the field-induced magnetic ordering is best described as the Bose-Einstein condensation (BEC) of spin triplets, with $S_z = 1$ called triplons. However, in the case of exchange disorder, the nature of the ground state in a magnetic field and the critical behavior of the field-induced magnetic ordering are not sufficiently understood, although there have been some studies on this problem.^{15–21}

In a magnetic field H that is comparable to the gap, the effective Hamiltonian of triplons is expressed as

$$\mathcal{H} = \sum_i (J_i - g\mu_B H) a_i^\dagger a_i + \sum_i \sum_j t_{ij} a_i^\dagger a_j + \frac{1}{2} \sum_i \sum_j U_{ij} a_i^\dagger a_j^\dagger a_j a_i. \quad (1)$$

The first, second, and third terms denote the local potential, hopping, and interaction of triplons, respectively. The intradimer exchange interaction J_i on dimer site i corresponds to the local potential of triplons, $V_i = J_i - g\mu_B H$. The ground state and the quantum phase transition for lattice bosons in a random potential were investigated theoretically by Fisher *et al.*²² They argued that a new phase called a Bose glass (BG) emerges as a ground state, in addition to BEC and Mott insulating (MI) phases, which correspond to the ordered phase and gapped phase in the magnetic system, respectively. Bosons are localized in the BG phase because of randomness, but there is no gap; thus, the compressibility is finite. Fisher *et al.* showed that the BEC transition occurs only from the BG phase, and that near $T = 0$, the relation between transition temperature T_c and boson density ρ is expressed as $T_c \sim [\rho_s(0)]^y$, $\rho_s(0) \sim (\rho - \rho_c)^\zeta$, where ρ_c is the critical density at which the BEC transition occurs and $\rho_s(0)$ is the condensate density at $T = 0$. The exponents y and ζ are given by $y = 3/4$ and $\zeta \geq 8/3$ in the case of three dimensions. The critical behavior is different from that of the standard BEC case

without randomness, for which these exponents are $y = 2/3$ and $\zeta = 1$.

Recent theory has demonstrated the emergence of the BG phase in a disordered quantum magnet.^{17,18} The BG phase has also been studied in other disordered quantum systems, such as ⁴He adsorbed on porous Vycor glass,^{22,23} amorphous superconductors,²⁴ and trapped cold atoms.²⁵ From the correspondence between the boson density and the magnetization in the coupled spin-dimer system, the relation $(\rho - \rho_c) \propto (H - H_c)$ is obtained, where H_c is the critical magnetic field of the triplon BEC. Hence, for the coupled spin-dimer system with exchange disorder, the transition field $H_N(T)$ near $T = 0$ should be expressed by the power law

$$[H_N(T) - H_c] \propto T^\phi, \quad (2)$$

with the critical exponent $\phi \leq 1/2$. Consequently, the low-temperature phase boundary should be tangential to the field axis at $T = 0$, as shown in Fig. 1(a). This phase boundary behavior is qualitatively different from that of a pure system, for which $\phi = 3/2$, and thus the phase boundary is perpendicular to the field axis. The H_B in Fig. 1(a) is the critical field for the MI-BG transition. The BG phase exists between H_B and H_c .

To investigate the triplon BEC under the effect of the localization, we performed specific heat and electron spin resonance (ESR) measurements on $\text{Tl}_{1-x}\text{K}_x\text{CuCl}_3$. The parent compounds TiCuCl_3 and KCuCl_3 have the same crystal structure, which is composed of the chemical dimer Cu_2Cl_6 , in which Cu^{2+} has spin-1/2. Their magnetic ground states are spin singlets with excitation gaps of 7.5 and 31 K, respectively.²⁶ The gaps originate from the strong antiferromagnetic exchange interaction between spins in the chemical dimer. The neighboring spin dimers couple antiferromagnetically in three dimensions. The intradimer exchange interaction was evaluated to be $J/k_B = 65.9$ and 50.4 K for TiCuCl_3 and KCuCl_3 , respectively.^{27–29} Because these two intradimer interactions are different, the partial K⁺ ion substitution for Tl⁺ ions produces the random local potential V_i of the triplon.³⁰

Single crystals of $\text{Tl}_{1-x}\text{K}_x\text{CuCl}_3$ were synthesized from a melt comprising a mixture of TiCuCl_3 and KCuCl_3 in the ratio of $1 - x$ to x . The potassium concentration x was determined by inductively coupled plasma optical emission

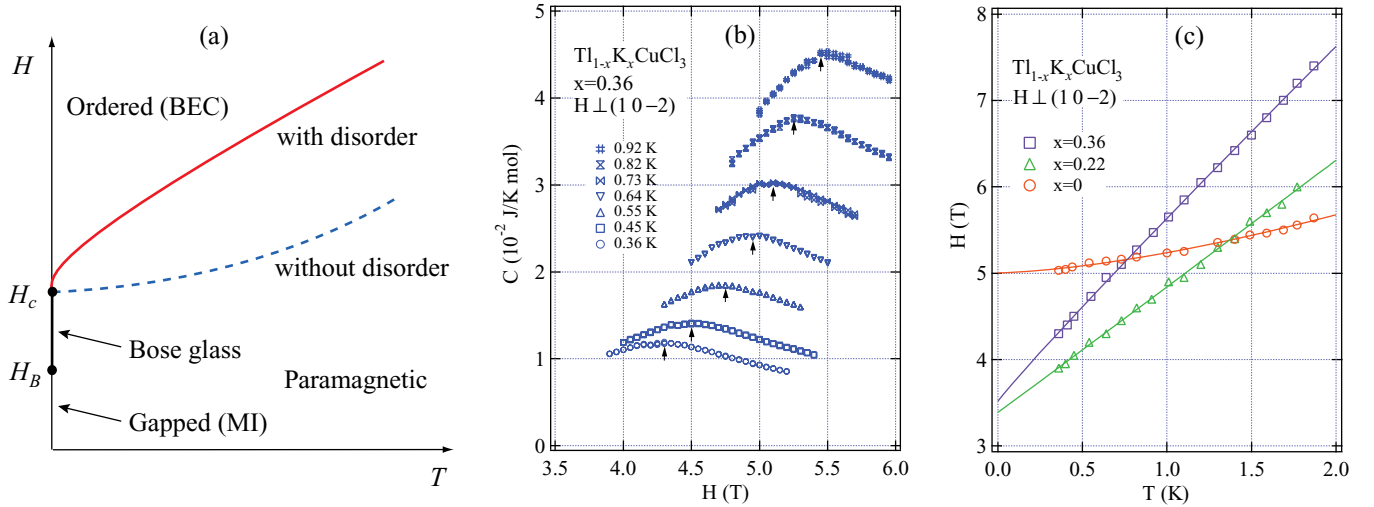


FIG. 1. (Color online) (a) Schematic low-temperature phase boundaries expected for $\text{Tl}_{1-x}\text{K}_x\text{CuCl}_3$. Solid and dashed lines denote the boundaries for $x \neq 0$ and $x = 0$, respectively. For simplification, the critical fields H_c for both cases are plotted at the same position. (b) Field scans of the specific heat in $\text{Tl}_{1-x}\text{K}_x\text{CuCl}_3$ with $x = 0.36$ measured at various temperatures. Arrows denote the transition field $H_N(T)$. (c) Magnetic field vs temperature diagram obtained below 2 K for $x = 0, 0.22$, and 0.36 . Solid lines denote the fits by Eq. (2) for $T < 2$ K.

spectrochemical analysis at the Center for Advanced Materials Analysis, Tokyo Institute of Technology (TIT). The specific heat was measured down to 0.36 K in magnetic fields of up to 9 T using a physical property measurement system (Quantum Design PPMS) by the relaxation method. High-frequency, high-field ESR measurements were performed using the terahertz ESR apparatus (TESRA-IMR)³¹ at the Institute for Material Research, Tohoku University. The temperature of the sample was lowered to 0.55 K using liquid ^3He . A magnetic field was applied using a multilayer pulse magnet. In all the present experiments, the magnetic field was applied perpendicular to the cleavage $(1,0,\bar{2})$ plane, because the magnetic anisotropy in this plane is so small that the $U(1)$ symmetry is approximately conserved.³²

The specific heat obtained from a temperature scan exhibits a small cusplike anomaly owing to magnetic ordering for $H \geq 4.5$ T. The anomaly becomes smaller with decreasing magnetic field. Thus, we performed a field scan of the specific heat at various temperatures below 2 K. Some examples of the measurements for $x = 0.36$ are shown in Fig. 1(b). The specific heat exhibits a cusplike anomaly, to which we assign the transition field $H_N(T)$. The transition field is well defined within an error of ± 0.1 T. The phase transition points obtained below 2 K for $x = 0, 0.22$, and 0.36 are summarized in Fig. 1(c). It is clear that the critical behaviors of the phase boundaries for $x = 0$ and $x \neq 0$ near $T = 0$ are qualitatively different. The phase boundary for $x = 0$ is normal to the field axis for $T \rightarrow 0$ but it is not for $x \neq 0$.

To investigate the critical behavior, we fit the power law given by Eq. (2) taking both ϕ and H_c as fitting parameters. For $x = 0$, we obtain $\phi = 1.53 \pm 0.14$ and $H_c = 5.00 \pm 0.02$ T using the data for $0.35 \leq T < 2$ K. The solid line for $x = 0$ in Fig. 1(c) is the fit with $\phi = 1.53$. This critical exponent ϕ coincides with $\phi_{\text{BEC}} = 3/2$ predicted by the BEC theory without disorder.^{4,9,10,22} On the other hand, for $x = 0.22$ and 0.36 , we obtain $\phi = 1.01 \pm 0.05$ and 0.96 ± 0.03 , respectively, using all the data below 2 K. The solid lines

for $x = 0.22$ and 0.36 in Fig. 1(c) are the fits with these exponents. However, for $x \neq 0$, the critical exponent ϕ tends to decrease with decreasing fitting window. Thus, we analyze the critical behavior of the phase boundary for $x = 0.36$ in detail. We fit Eq. (2) in the temperature range of $T_{\min} \leq T \leq T_{\max}$, setting the lowest temperature at $T_{\min} = 0.36$ K and varying the highest temperature T_{\max} from 1.87 to 0.82 K. The critical exponent ϕ as a function of T_{\max} is shown in Fig. 2. The critical exponent ϕ decreases monotonically with decreasing T_{\max} , and $\phi = 0.58 \pm 0.17$ with $H_c = 2.7 \pm 0.6$ T for $T_{\max} = 0.82$ K. The solid line in Fig. 2 is the fit with these ϕ and H_c . With decreasing T_{\max} used for fitting, the critical exponent ϕ shows a clear tendency to reach a value smaller than $1/2$, although the convergence of ϕ is not observed in the present temperature range. This critical behavior is consistent with that for the BG-BEC transition discussed by Fisher *et al.*²² The similar behavior for the critical exponent is also observed for $x = 0.22$.

As shown in Fig. 1(c), the critical fields H_c for $x = 0.22$ and 0.36 are smaller than that for $x = 0$. This should be mainly owing to the fact that the average intradimer interaction decreases with increasing x . Within the framework of the dimer mean-field approximation,⁶ the triplet gap is expressed as $\Delta = [J(J - 2|\tilde{J}|)]^{1/2}$, where \tilde{J} is expressed by a linear combination of interdimer interactions.⁶ The gap shrinks either when the intradimer interaction J is reduced or when the interdimer interaction is enhanced. The temperature T_M giving the maximum magnetic susceptibility decreases with increasing x , as shown in Fig. 1 in Ref. 15. This indicates that the average intradimer interaction decreases with x , because T_M is given by $1.60T_M = J/k_B$, according to the mean-field approximation.

To investigate the triplon localization, we performed ESR measurements on $\text{Tl}_{1-x}\text{K}_x\text{CuCl}_3$ with $x = 0.22$ and 0.36 . The crystals used in the specific heat and ESR measurements were taken from the same batch. We used thick samples to increase the intensity. The measurements were performed

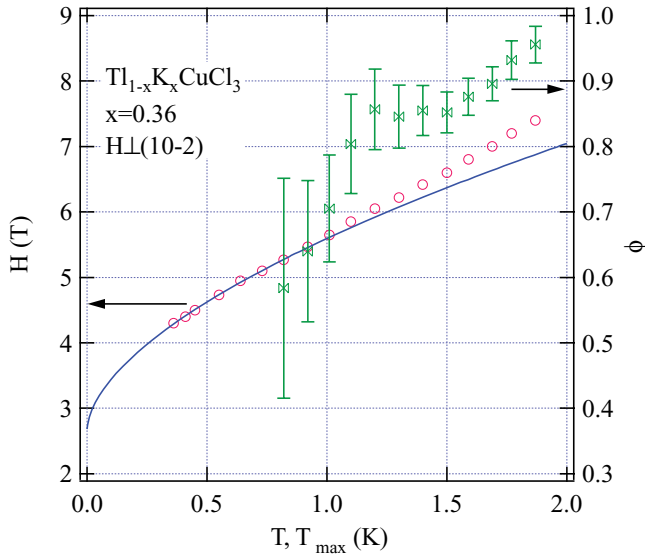


FIG. 2. (Color online) Low-temperature phase boundary for $x = 0.36$ and critical exponent ϕ as a function of T_{\max} obtained by fitting Eq. (2) to transition points between 0.36 K and T_{\max} . The solid line is the fit with $\phi = 0.58$ and $H_c = 2.7$ T.

mainly at frequencies of 111 and 118.6 GHz for $x = 0.22$ and 0.36 , respectively. The paramagnetic resonance fields for these frequencies were estimated to be 3.55 and 3.80 T, respectively, using $g = 2.23$ for $H \perp (1,0,\bar{2})$. The resonance field H_0 is close to the critical field H_c . A single ESR line with a width of ~ 0.1 T was observed in the paramagnetic phase for $0.55 \leq T \leq 16$ K. The signal intensity below 4 K is much larger than that of the paramagnetic resonance for pure TiCuCl_3 with a gapped ground state.³² Although the signal intensity decreases monotonically with decreasing temperature, the intensity is sufficient, even at the lowest temperature, to analyze the line shape as shown in Fig. 3. We also measured the ESR spectrum at 102 GHz, but we could not obtain a well-defined signal to analyze the line shape.

In the paramagnetic phase, the linewidth is produced by the local field owing to perturbations that do not commute with

the total spin such as the anisotropic exchange, the dipolar interaction, and the Zeeman interaction with nonuniform g factors. From a statistical point of view, it is natural to assume that the local field has a Gaussian distribution.^{33,34} Thus, when the triplons that are created on the dimers localize, the line shape should be Gaussian, because the distribution of the local field determines the line shape of the ESR spectrum. On the other hand, if the triplons delocalize in the crystal, the local field acting on the spins is rapidly averaged, so that the ESR spectrum is narrowed and becomes Lorentzian.^{33,34} This is called exchange narrowing.

The raw ESR spectrum is somewhat unsymmetrical with respect to the resonance field H_0 , as shown in Fig. 3(a). This should be owing to the interference of the submillimeter wave inside the sample, because the wavelength of the submillimeter wave used and the sample thickness have the same order. Because the present system is an insulator, this unsymmetrical line shape is not intrinsic to the sample. Thus, we symmetrized the spectrum by averaging both sides of H_0 , i.e., we used $\{I(H) + I(2H_0 - H)\}/2$ as the intensity $I(H)$ at H . The symmetrized spectrum has a flat baseline. To analyze the line shape of these ESR spectra, we plotted $I(H_0)/I(H)$ against $[(H - H_0)/(\Delta H)]^2$, where ΔH is the linewidth at $I(H_0)/2$.³⁵ When the line shape is Gaussian, $I(H_0)/I(H)$ increases exponentially, while for the Lorentzian line shape, $I(H_0)/I(H)$ is a linear function of $[(H - H_0)/(\Delta H)]^2$ with a slope of unity, as shown by dashed and solid lines, respectively, in Figs. 3(b) and 3(c). The $I(H_0)/I(H)$ vs $[(H - H_0)/(\Delta H)]^2$ plots at various temperatures for $x = 0.36$ and 0.22 are shown in Figs. 3(b) and 3(c), respectively. We can see a similar temperature variation in both figures. The $I(H_0)/I(H)$ at high temperatures is almost linear in $[(H - H_0)/(\Delta H)]^2$ with a slope of unity, which indicates a Lorentzian line shape. On the other hand, at sufficiently low temperatures, the $I(H_0)/I(H)$ vs $[(H - H_0)/(\Delta H)]^2$ plot is between the Lorentzian and Gaussian plots. Such an ESR line shape is observed in one-dimensional Heisenberg antiferromagnets, in which the time correlation function of the local fields acting on the spins is not damped rapidly but has a long time tail.³⁵

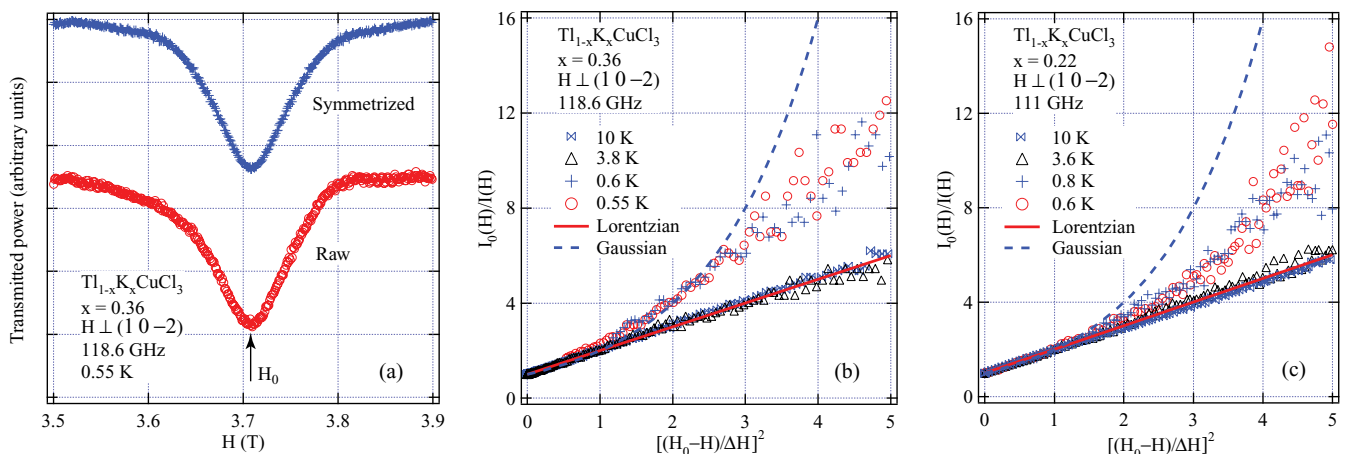


FIG. 3. (Color online) (a) ESR spectra for $x = 0.36$ observed at 0.55 K for 118.6 GHz. Lower and upper spectra are raw and symmetrized spectra, respectively. $I(H_0)/I(H)$ vs $[(H - H_0)/(\Delta H)]^2$ plots for the ESR spectra measured at various temperatures (b) for $x = 0.36$ and (c) for $x = 0.22$. Solid and dashed lines are the same plots assuming Lorentzian and Gaussian functions, respectively.

In the present temperature range, the BEC phase is not reached even at the lowest temperature. At high temperatures, the thermal hopping of triplons is activated. This causes rapid averaging of the local fields, which leads to a narrowed Lorentzian line shape. At sufficiently low temperatures, the thermal effect is suppressed. Thus, the intermediate line shape observed for $T \leq 0.8$ K can be attributed to the localization of triplons. Because the resonance fields for 111 and 118.6 GHz are close to the critical field H_c , it is considered that the complete localization does not occur in the present temperature range; thus, the line shape is intermediate between Gaussian and Lorentzian functions.

Oosawa and Tanaka¹⁵ reported the results of magnetization measurements on $Tl_{1-x}K_xCuCl_3$ with $x \leq 0.36$. The magnetization curve that they observed at $T = 1.8$ K had a finite slope even for $H < H_c$. This was not ascribed to the finite-temperature effect, because pure $TlCuCl_3$ exhibits almost zero magnetization up to the critical field H_c . This result indicates that the magnetic susceptibility $\chi = \partial M / \partial H$ for $H < H_c$ is finite in the ground state. Because the magnetic susceptibility corresponds to the compressibility of the lattice boson system $\kappa = \partial \rho / \partial \mu$, where μ is the chemical potential, the finite magnetic susceptibility for $T \rightarrow 0$ means that the compressibility of the ground state is finite. In the low-field

phase below H_c , long-range magnetic ordering is absent in spite of the finite susceptibility. These properties for $H < H_c$ are consistent with the characteristics of the BG phase.²² From these observations and the present ESR results, we can deduce that the ground state for $H < H_c$ in $Tl_{1-x}K_xCuCl_3$ is the BG phase of triplons. The gapped MI phase for $H < H_B$ appears to be destroyed in the present system.

In conclusion, from the analysis of the phase transition data and the line shape of the ESR spectrum for $Tl_{1-x}K_xCuCl_3$ combined with the previous result for magnetization measurement, we deduce that the quantum phase transition at H_c is the BG-BEC transition of triplons and that the critical behavior for the temperature dependence of the transition field near H_c is described by the small-exponent characteristic of the BG-BEC transition.²²

We express our sincere thanks to M. Oshikawa, T. Suzuki, A. Oosawa, and T. Goto for discussions and comments. This work was supported by a Grant-in-Aid for Scientific Research (A) from Japan Society for the Promotion of Science (JSPS), and the Global COE Program “Nanoscience and Quantum Physics” at TIT funded by the Ministry of Education, Culture, Sports, Science and Technology of Japan.

¹T. M. Rice, *Science* **298**, 760 (2002).

²T. Giamarchi, Ch. Rüegg, and O. Tchernyshyov, *Nat. Phys.* **4**, 198 (2008).

³A. Oosawa, M. Ishii, and H. Tanaka, *J. Phys. Condens. Matter* **11**, 265 (1999).

⁴T. Nikuni, M. Oshikawa, A. Oosawa, and H. Tanaka, *Phys. Rev. Lett.* **84**, 5868 (2000).

⁵Ch. Rüegg, N. Cavadini, A. Furrer, H.-U. Güdel, K. Krämer, H. Mutka, A. Wildes, K. Habicht, and P. Vorderwisch, *Nature (London)* **423**, 62 (2003).

⁶A. Oosawa, T. Takamasu, K. Tatani, H. Abe, N. Tsujii, O. Suzuki, H. Tanaka, G. Kido, and K. Kindo, *Phys. Rev. B* **66**, 104405 (2002).

⁷M. Jaime, V. F. Correa, N. Harrison, C. D. Batista, N. Kawashima, Y. Kazuma, G. A. Jorge, R. Stein, I. Heinmaa, S. A. Zvyagin, Y. Sasago, and K. Uchinokura, *Phys. Rev. Lett.* **93**, 087203 (2004).

⁸M. Matsumoto, B. Normand, T. M. Rice, and M. Sigrist, *Phys. Rev. B* **69**, 054423 (2004).

⁹N. Kawashima, *J. Phys. Soc. Jpn.* **73**, 3219 (2004).

¹⁰G. Misguich and M. Oshikawa, *J. Phys. Soc. Jpn.* **73**, 3429 (2004).

¹¹M. B. Stone, C. Broholm, D. H. Reich, P. Schiffer, O. Tchernyshyov, P. Vorderwisch, and N. Harrison, *New J. Phys.* **9**, 31 (2007).

¹²F. Yamada, T. Ono, H. Tanaka, G. Misguich, M. Oshikawa, and T. Sakakibara, *J. Phys. Soc. Jpn.* **77**, 013701 (2008).

¹³R. Dell’Amore, A. Schilling, and K. Krämer, *Phys. Rev. B* **78**, 224403 (2008).

¹⁴T. Dodds, B.-J. Yang, and Y. B. Kim, *Phys. Rev. B* **81**, 054412 (2010).

¹⁵A. Oosawa and H. Tanaka, *Phys. Rev. B* **65**, 184437 (2002).

¹⁶Y. Shindo and H. Tanaka, *J. Phys. Soc. Jpn.* **73**, 2642 (2004).

¹⁷O. Nohadani, S. Wessel, and S. Haas, *Phys. Rev. Lett.* **95**, 227201 (2005).

¹⁸T. Roscilde and S. Haas, *J. Phys. B* **39**, S153 (2006).

¹⁹T. Goto, T. Suzuki, K. Kanada, T. Saito, A. Oosawa, I. Watanabe, and H. Manaka, *Phys. Rev. B* **78**, 054422 (2008).

²⁰T. Suzuki, F. Yamada, T. Kawamata, I. Watanabe, T. Goto, and H. Tanaka, *Phys. Rev. B* **79**, 104409 (2009).

²¹T. Hong, A. Zheludev, H. Manaka, and L.-P. Regnault, *Phys. Rev. B* **81**, 060410(R) (2010).

²²M. P. A. Fisher, P. B. Weichman, G. Grinstein, and D. S. Fisher, *Phys. Rev. B* **40**, 546 (1989).

²³B. C. Crooker, B. Hebral, E. N. Smith, Y. Takano, and J. D. Reppy, *Phys. Rev. Lett.* **51**, 666 (1983).

²⁴S. Okuma, S. Shinozaki, and M. Morita, *Phys. Rev. B* **63**, 054523 (2001).

²⁵L. Fallani, J. E. Lye, V. Guarrera, C. Fort, and M. Inguscio, *Phys. Rev. Lett.* **98**, 130404 (2007).

²⁶W. Shiramura, K. Takatsu, H. Tanaka, M. Takahashi, K. Kamishima, H. Mitamura, and T. Goto, *J. Phys. Soc. Jpn.* **66**, 1900 (1997).

²⁷N. Cavadini, W. Henggeler, A. Furrer, H.-U. Güdel, K. Krämer, and H. Mutka, *Eur. Phys. J. B* **7**, 519 (1999).

²⁸N. Cavadini, G. Heigold, W. Henggeler, A. Furrer, H.-U. Güdel, K. Krämer, and H. Mutka, *Phys. Rev. B* **63**, 172414 (2001).

²⁹A. Oosawa, T. Kato, H. Tanaka, K. Kakurai, M. Müller, and H.-J. Mikeska, *Phys. Rev. B* **65**, 094426 (2002).

³⁰This partial ion substitution produces not the binomial distribution for V_i but a continuous distribution, because the configuration of K^+ and Tl^+ ions around the chemical dimer Cu_2Cl_6 determines the intradimer interaction.

³¹H. Nojiri, Y. Ajiro, T. Asano, and J. P. Boucher, *New J. Phys.* **8**, 218 (2006).

³²V. N. Glazkov, A. I. Smirnov, H. Tanaka, and A. Oosawa, *Phys. Rev. B* **69**, 184410 (2004).

³³P. W. Anderson and P. R. Weiss, *Rev. Mod. Phys.* **25**, 269 (1953).

³⁴R. Kubo and K. Tomita, *J. Phys. Soc. Jpn.* **9**, 45 (1954).

³⁵R. E. Dietz, F. R. Merritt, R. Dingle, D. Hone, B. G. Silbernagel, and P. M. Richards, *Phys. Rev. Lett.* **26**, 1186 (1971).